

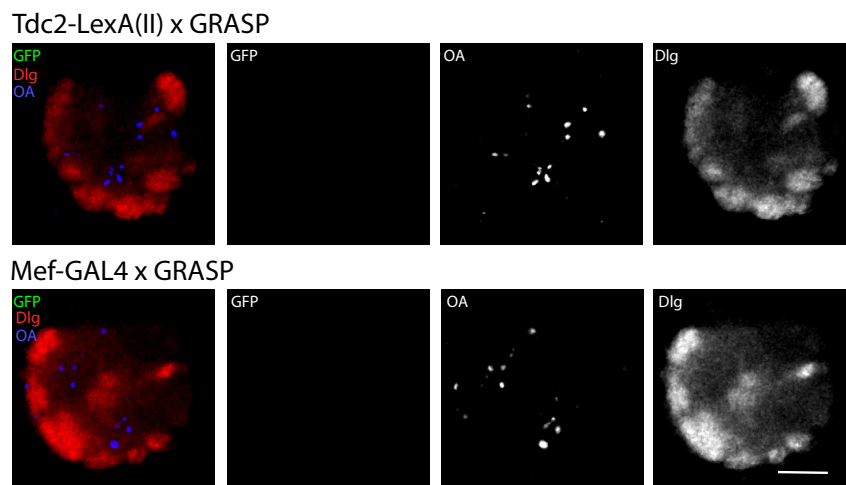
Octopaminergic neurons have multiple targets in *Drosophila* larval mushroom body calyx and can modulate behavioral odor discrimination

J Y Hilary Wong¹, Bo Angela Wan¹, Tom Bland, Marcella Montagnese, Alex D McLachlan, Cahir J O’Kane, Shuo Wei Zhang, Liria M Masuda-Nakagawa*

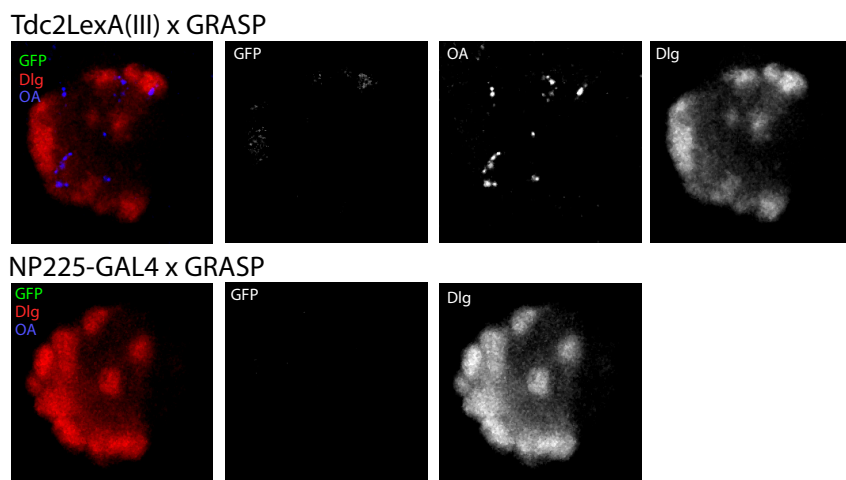
Supplementary Figure Legends

Supplementary Fig. 1. LexA or GAL-4 GRASP controls. To verify that only puncta of reconstituted GFP were detected in GRASP experiments, a line carrying GRASP constructs *UAS-CD4::spGFP1-10* and *LexAop-CD4::spGFP11*, as used in Fig. 3, was crossed to single *LexA* or *GAL4* insertions as shown, and GRASP signals were detected in the larval progeny. Panels show sections of calyces of 3rd instar larvae, labeled with monoclonal rat anti-GFP, anti-DLG, and anti-octopamine. **A.** Top row: *Tdc2-LexA(II)*, bottom row *Mef2-GAL4*. Intensity levels for image processing were adjusted to the same levels as Fig 3C. Note the complete absence of GFP puncta. **B.** Top row is *Tdc2(III)*; bottom row is *NP225-GAL4*. Note the complete absence of GFP puncta for *Tdc2-LexA(III)*; only an occasional smear over glomeruli was observed when maximum intensity was adjusted to the same levels as Fig. 3B (*NP225-GAL4 + Tdc2-LexA (III)*). GFP signal was completely absent from *NP225-GAL4* GRASP when intensity levels were adjusted to the same values as Fig. 3B. Scale bar is 10 μ m.

A



B



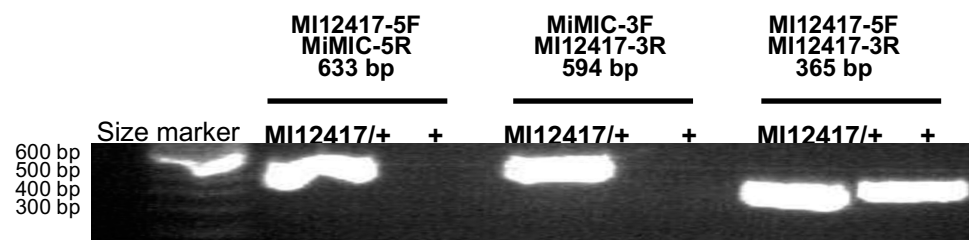
Supplementary Fig. 2. PCR verification of *MI12417(Oamb)* insertion in the *Oamb* gene.

(A) Primers designed against 5' (*MI12417-5F/MiMIC-5R*) and 3' (*MiMIC-3F/MI12417-3R*) *MiMIC* insertion flanking ends were used to validate the *MI12417* insertion in the *Oamb* gene. **(B)** PCR results for *MI12417* *MiMIC* insertion. PCR products were detected for *MI12417* 5' and 3' flanking ends using *MI12417* DNA template, but not for the negative control template (denoted as +). A PCR product was detected using primers against the *Oamb* genomic flanking sequences (*MI12417-5F/MI12417-3R*) for the negative control lacking *MI12417* insertion, as well as for *MI12417* due to heterozygosity of the insertion. Abbreviations: MiL/MiR, *MiMIC* insertion ends Left/Right. SA, Splice Acceptor Site.

A



B



Supplementary Fig. 3. Alignment of *MI12417* 5' flanking PCR products to MiMIC and *Oamb* genomic sequences. (A) Sequenced 5' *MI12417* PCR product. Alignment to MiMIC sequences is indicated in yellow, alignment to *Oamb* in grey. Overlapping alignment at the MiMIC insertion site (TA) indicated in red. (B-C) Alignment of *MI12417* 5' PCR products to MiMIC (B) and *Drosophila melanogaster* (C) sequences using Nucleotide BLAST (Altschul et al., 1990).

A. Sequence of *MI12417* 5' flanking end

```
NTCTTATT CGATAATATAAACATGGCTCAAAGAAGAAGTCACGCATCATAATTAG
CATTATATTCCAAGTTGGGCAAAAACAAGAAATCGATAAACGCTGAGGAAGCACATCAA
CAAATCGGCTTAGATAAAAATTGAGGTGGGATTAAATAGGAGCCGGATTCCAGCCAGAAA
ATGGCAGACATGAAAGCGAGCCATCGGCTAAACGAAATAAAATTATACGAGCCCCAACCA
CTATTAAATT CGAACAGCATGTTTTTGCA GTGCGCAATGTTAACACACTATATTATCA
ATACTACTAAAGATAACACATACCAATGCATTCGTCTCAAAGAGAATT TATTCTCTTC
ACGACGAAAAAAAAGTTTGCTCTATTCAACAAACAACAAAATATGAGTAATT ATT
CAAACGGTTTGCTTAAGAGATAAGAAAAAGTGACCACTATTAAATT CGAACGCGCGTAA
GCTACTAAATCTCTCANGAA
```

B. *MI12417* 5' flanking end alignment with *Oamb*

>AE014297.3 *Drosophila melanogaster* chromosome 3R Length=32079331

Features in this part of subject sequence:

- octopamine receptor in mushroom bodies, isoform D
- octopamine receptor in mushroom bodies, isoform G

Strand=Plus/Minus

Query 71	CAAGTTGGCAAAAACAAGAAATCGATAAACGCTGAGGAAGCACATCAAACAAATCGGCT	130
Sbjct 20697214	CAAGTTGGCAAAAACAAGAAATCGATAAACGCTGAGGAAGCACATCAAACAAATCGGCT	20697155
Query 131	TAGATAAAATTGAGGTGGATTAAATAGGAGCGGGATTCCAGCCAGAAAATGGCAGACA	190
Sbjct 20697154	TAGATAAAATTGAGGTGGATTAAATAGGAGCGGGATTCCAGCCAGAAAATGGCAGACA	20697095
Query 191	TGAAAGCGAGCCATCGGCTAAAACGAAATAAAATATA	227
Sbjct 20697094	TGAAAGCGAGCCATCGGCTAAAACGAAATAAAATATA	20697058

C. *MI12417* 5' flanking end alignment with MiMIC sequences

>GU370067.1 Synthetic construct MiMIC transposable element, complete sequence Length=7267

Strand=Plus/Plus

Query 226	TACGAGCCCCAACCACTATTAAATT CGAACAGCATGttttttGCAGT GCGCAATGTTAA	285
Sbjct 102	TACGAGCCCCAACCACTATTAAATT CGAACAGCATGTTTTTGCA GTGCGCAATGTTAA	161
Query 286	CACACTATATTCAATACTAAAGATAACACATACCAATGCATTCGTCTCAAAGAG	345
Sbjct 162	CACACTATATTCAATACTAAAGATAACACATACCAATGCATTCGTCTCAAAGAG	221
Query 346	AATTTTATTCTCTTACGACGaaaaaaaaaaaaGTTTGCTCTATTCCAAACAACAAAAAA	405
Sbjct 222	AATTTTATTCTCTTACGACGaaaaaaaaaaaaGTTTGCTCTATTCCAAACAACAAAAAA	281
Query 406	TATGAGTAATTATTCAAACGGTTGCTTAAGAGATAAGAAAAAGTGACCACTATTAAAT	465
Sbjct 282	TATGAGTAATTATTCAAACGGTTGCTTAAGAGATAAGAAAAAGTGACCACTATTAAAT	341

Supplementary Fig. 4. Alignment of 3' flanking PCR products from *MI12417* to MiMIC and *Oamb* genomic sequences **(A)** Sequenced 3' *MI12417* PCR product. Alignment to MiMIC sequences is indicated in yellow, alignment to *Oamb* sequences in grey. Overlapping alignment at the MiMIC insertion site (TA) indicated in red. **(B-C)** Alignment of *MI12417* 3' PCR products to MiMIC **(B)** and *Drosophila melanogaster* **(C)** sequences using Nucleotide BLAST (Altschul et al., 1990).

A. Sequence of *MI12417* 3' flanking end

```

GCGGGAGTCGCGACTACCCCCACTGAGAGACTCAAAGGTTACCCAGTTGGGCCT
ACTCCCAGAAACCGCTTGTGACCTGGCCGCGGGGGAAATTAAATTATTGTTTAA
GTATGATAGTAAATCACATTACGCCGTTGGAATTAAATAGTGGTCACTTTTCTTATC
TCTTAAGCAACCGTTGAATAAATTACTCATATTGTTGTTGGAAATAGAGCAA
AACTTTTTTTTCGTCGTGAAGAGAAATAAATTCTTGTGAGACGAAATGCATTGGTATG
TGTATCTTAGTAGTATTGATAATATAGTGTGTTAACATTGCCACTGCAAAAAAAAC
ATGCTGTTGAAATTAAATAGTGGTGGGGCTCGTAATATGTCCTCCCTGTTAGCATGTTCT
GTTGCAATTCTATTCTTAGGTTTGTCGTTCTGAGGCTCACTGGTCCCCAAAGA
CTCTGTGGGGCGGATAATCGGCTTGTGACAGCCGTTTGCTGGCTGAATGT
TTAACACACTGGACCATCAGTTGACTCAGGACTCACGGACAGTGGCTCCTCTCAA
AGAGAGTTTATTCTCTGCCACAGCAAGGAAGGCCCTGACATGTCGAACAGGACCC
CGTGTGGCTCATCTTGTGCTCTGTGGGAGGCAAGTCTAACCCAGTGTGACCTCCATGAA
GTCGAGAACAGTAACTCAATCTCCATCCCACCCATTGCTGCCAGACCGTGAGGA
GCCACCTCCGGTGGACAC

```

B. *MI12417* 3' flanking end alignment with MiMIC sequences

```

>AE014297.3 Drosophila melanogaster chromosome 3R      Length=32079331
Features in this part of subject sequence:
    octopamine receptor in mushroom bodies, isoform D
    octopamine receptor in mushroom bodies, isoform G

>GU370067.1 Synthetic construct MIMIC transposable element, complete sequence      Length=7267
Strand=Plus/Plus
Query  252   tCGTCGTGAAGAGAATAAAATTCTCTTGAGACGAAATGCATTGGTATGTGTTATCTTA  311
           ||||||| ||||||| ||||||| ||||||| ||||||| ||||||| ||||||| ||||||| |||||
Sbjct  7062   TCGTCGTGAAGAGAATAAAATTCTCTTGAGACGAAATGCATTGGTATGTGTTATCTTA  7121

Query  312   GTAGTATTGATAATATAGTGTGTTAACATTGCCACTGCaaaaaaaaaCATGCTGTTGA  371
           ||||||| ||||||| ||||||| ||||||| ||||||| ||||||| ||||||| ||||||| |||||
Sbjct  7122   GTAGTATTGATAATATAGTGTGTTAACATTGCCACTGCAAAAAAAACATGCTGTTGA  7181

Query  372   ATTAATAGTGGTGGGGCTCGTA  394
           ||||||| ||||||| ||||||| |||||
Sbjct  7182   ATTAATAGTGGTGGGGCTCGTA  7204

```

C. *MI12417* 3' flanking end alignment with *Oamb* sequences

```

>AE014297.3 Drosophila melanogaster chromosome 3R      Length=32079331
Features in this part of subject sequence:
    octopamine receptor in mushroom bodies, isoform D
    octopamine receptor in mushroom bodies, isoform G

Strand=Plus/Minus
Query  393   TAATATGTCCTCCCTGTTAGCATGTTCTGTTGCAATTCTATTTCTTAGGTTTTGT  452
           ||||||| ||||||| ||||||| ||||||| ||||||| ||||||| ||||||| ||||||| |||||
Sbjct  20697059  TAATATGTCCTCCCTGTTAGCATGTTCTGTTGCAATTCTATTTCTTAGGTTTTGT  20697000

Query  453   CGTTTCAGGCCTCACTGGTCCCCAAAGACTCTGTGGGGCCGATAATC  500
           ||||||| ||||||| ||||||| ||||||| ||||| ||| ||| ||| |
Sbjct  20696999  CGTTTCAGGCCTCACTGGTCCCCAAAGACGCTGTGGTGGCG-ATAATC  20696953

```

Supplementary Fig. 5. *MI12417* is inserted in coding intron 3 of *Oamb*. **(A)** Extract of TBLASTN query of Oamb-B against the *Drosophila* genome assembly, showing an intron at coordinates 20693849–20698333, inserted at amino-acid residue 338 of Oamb-B. **(B)** Extract of BLASTN search of *Oamb-B* RNA, showing a splice site between nucleotides 2007 and 2008. **(C)** Alignment of Oamb-B protein and Oamb-B RNA sequences around the third intron, highlighting residue G338 and the AGGG splice site in yellow. **(D)** Map of *MI12417* insertion (3R:20,697,059) relative to *Oamb* gene and transcripts (Adapted from GBrowse, www.flybase.org).

A

Oamb-B:	284	PWKCELTNDRGYVLYSALGSFYIPMFVMLFFYWRIYRAAVRTTRAINQGFKTTKG	338
		PWKCELTNDRGYVLYSALGSFYIPMFVMLFFYWRIYRAAVRTTRAINQGFKTTKG	
Genome:	20698497	PWKCELTNDRGYVLYSALGSFYIPMFVMLFFYWRIYRAAVRTTRAINQGFKTTKG	20698333
Oamb-B:	338	GSPRESGNNRVDESQLILRIHGRPCSTPQRTPLSVHMSSTLSVNSNGGGGAVASGLG	397
		GSPRESGNNRVDESQLILRIHGRPCSTPQRTPLSVHMSSTLSVNSNGGGGAVASGLG	
Genome:	20693849	GSPRESGNNRVDESQLILRIHGRPCSTPQRTPLSVHMSSTLSVNSNGGGGAVASGLG	20693670

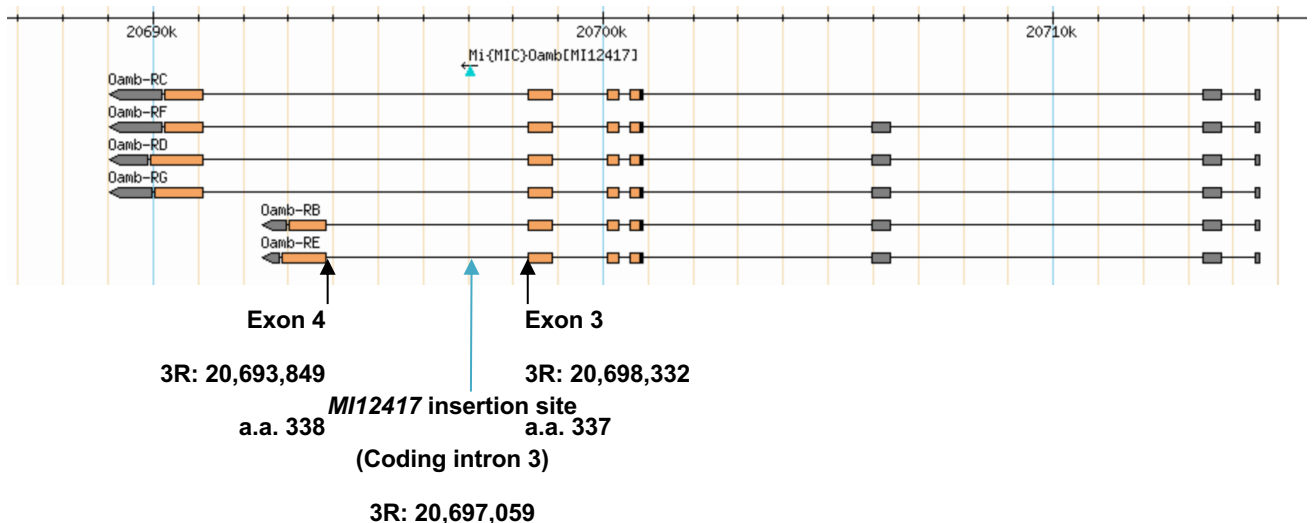
B

Oamb-B:	1964	TGAGAACGACGAGAGCCATCAACCAGGGCTTCAAGACCACCAAG	2007
Genome:	20698379	TGAGAACGACGAGAGCCATCAACCAGGGCTTCAAGACCACCAAG	20698332
Oamb-B:	2008	GGCAGTCCCCCGAGTCGGGCAACAATCGAGTGGACGAGTCCCAGCTCATATTGCGCATT	2067
Genome:	20693849	GGCAGTCCCCCGAGTCGGGCAACAATCGAGTGGACGAGTCCCAGCTCATATTGCGCATT	20693790

C

Coding intron 3; 3R:20,697,059
Exon 4>3R:20,693,848-20,692,947
 ATCAACCAGGGCTTCAAGACCACCAAGGGCAGTCCCCCGAGTCGGGCAACAATCGAGTG
 329 -I--N--Q--G--F--K--T--K--G--S--P--R--E--S--G--N--N--R--V-

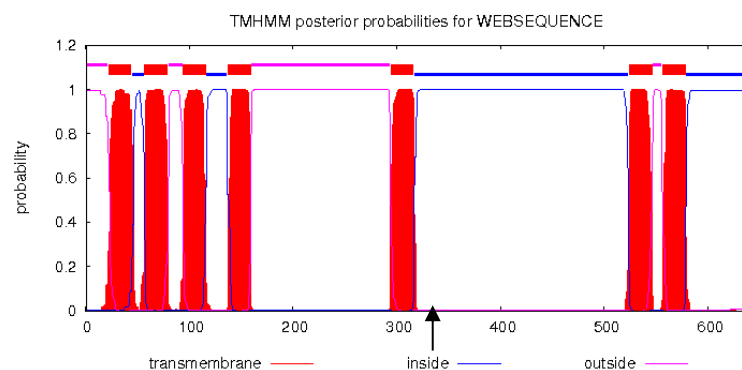
D



Supplementary Fig. 6. TMHMM predictions of transmembrane domains for Oamb-PB and PC isotypes. The third intracellular loop, where residue G338 is found, is highlighted in yellow.

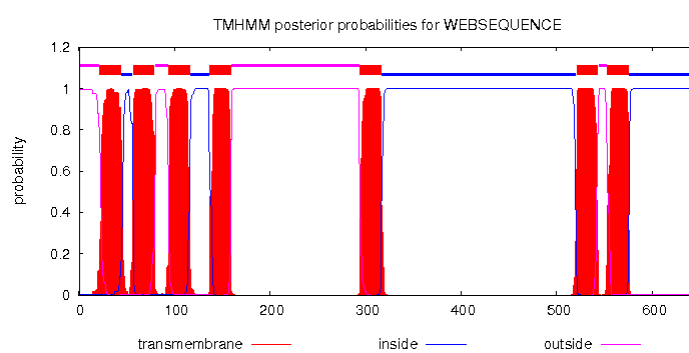
A. Oamb-PB TMHMM Predictions

WEBSEQUENCE	TMHMM2.0	outside	1	21
WEBSEQUENCE	TMHMM2.0	TMhelix	22	44
WEBSEQUENCE	TMHMM2.0	inside	45	56
WEBSEQUENCE	TMHMM2.0	TMhelix	57	79
WEBSEQUENCE	TMHMM2.0	outside	80	93
WEBSEQUENCE	TMHMM2.0	TMhelix	94	116
WEBSEQUENCE	TMHMM2.0	inside	117	136
WEBSEQUENCE	TMHMM2.0	TMhelix	137	159
WEBSEQUENCE	TMHMM2.0	outside	160	293
WEBSEQUENCE	TMHMM2.0	TMhelix	294	316
WEBSEQUENCE	TMHMM2.0	inside	317	523
WEBSEQUENCE	TMHMM2.0	TMhelix	524	546
WEBSEQUENCE	TMHMM2.0	outside	547	555
WEBSEQUENCE	TMHMM2.0	TMhelix	556	578
WEBSEQUENCE	TMHMM2.0	inside	579	637



B. Oamb-PC TMHMM Predictions

WEBSEQUENCE	TMHMM2.0	outside	1	21
WEBSEQUENCE	TMHMM2.0	TMhelix	22	44
WEBSEQUENCE	TMHMM2.0	inside	45	56
WEBSEQUENCE	TMHMM2.0	TMhelix	57	79
WEBSEQUENCE	TMHMM2.0	outside	80	93
WEBSEQUENCE	TMHMM2.0	TMhelix	94	116
WEBSEQUENCE	TMHMM2.0	inside	117	136
WEBSEQUENCE	TMHMM2.0	TMhelix	137	159
WEBSEQUENCE	TMHMM2.0	outside	160	293
WEBSEQUENCE	TMHMM2.0	TMhelix	294	316
WEBSEQUENCE	TMHMM2.0	inside	317	520
WEBSEQUENCE	TMHMM2.0	TMhelix	521	543
WEBSEQUENCE	TMHMM2.0	outside	544	552
WEBSEQUENCE	TMHMM2.0	TMhelix	553	575
WEBSEQUENCE	TMHMM2.0	inside	576	645



Supplementary Fig. 7. *Mi12417* insertion location relative to *Oamb* cDNA and protein sequences. cDNA and protein sequences were taken from the ENSEMBL database (Aken et al., 2016; <http://www.ensembl.org>) for representative *Oamb* transcript protein isotype B. The beginning and range of each exon, obtained from the ENSEMBL database, is annotated in yellow. Transmembrane domains are indicated in green. MiMIC insertion location site, listed on the Gene Disruption Project database, is annotated in light blue. Abbreviations: TM, transmembrane domain; a.a., amino acid

3R:20,700,845

Exon 1>3R:20,700,845-20,700,594

1 ATGAATGAAACAGAGTGCAGGAT
1 -M--N--E--T--E--C--E--D-

TM I: a.a.22-44

25 CTCATCAAATCTGTGAAATGGACCGAACGCCAATCTGATCTCCCTGGCGTACTCGAG
9 -L--I--K--S--V--K--W--T--E--P--A--N--L--I--S--L--A--V--L--E--

85 TTCATCAACGTTCTGGTCATCGTGGCAACTGCCTCGTATTGCCGCCGCTTCTGTTCG
29 F--I--N--V--L--V--I--G--G--N--C--L--V--I--A--A--V--F--C--S--

TM II: a.a.57-79

145 AATAAGTTGAGGAGTGTGACGAACCTTCTTATTGTCAACCTAGCTGTGGCCGATCTCTG
49 -N--K--L--R--S--V--T--N--F--F--I--V--N--L--A--V--A--D--L--I--

Exon 2>3R:20,700,331

205 GTGGGTTTGGCCGTCCTACCCTCTCAGCACCTGGGAAGTCTTCAAGGTTGGATATT
69 -V--G--L--A--V--L--P--F--S--A--T--W--E--V--F--K--V--W--I--F--

-20,700,095

TM III: a.a.94-116

265 GGCATCTGGTGCCGCATTTGGCTGGCTGTCGATGTCTGGATGTGACGGCATCGATC
89 -G--D--L--W--C--R--I--W--L--A--V--D--V--W--M--C--T--A--S--I--

325 CTGAATCTGTGCCATATCACTGGACCGCTATGTGGCGGTACACGACCCGTACCTAC
109 -L--N--L--C--A--I--S--L--D--R--Y--V--A--V--T--R--P--V--T--Y--

TM IV: a.a.137-159

385 CCAAGCATAATGCCACGAAGAACGCAAGTCCTTAATGCCGGCATTGGGTACTCTCA
129 -P--S--I--M--S--T--K--A--K--S--L--I--A--G--I--W--V--L--S--

Exon 3>3R:20,698,857-

445 TTTTTTATTGCTTCCGCCGCTAGTCGGCTGGAAGGATCAAAGGCGGTTATACAGCCG
149 -F--F--I--C--F--P--P--L--V--G--W--K--D--Q--K--A--V--I--Q--P--

20,698,335

505 ACCTATCAAAGGAAACCATAACGCTTACTACACCACGATGTCAAGCTGGAGGAT
169 -T--Y--P--K--G--N--H--T--L--Y--Y--T--T--T--M--S--S--E--D--

565 GGTCAACTAGGGTTAGATAGCATTAAGGACCAAGGGCAGGGCATCCTGCCTCCATCCCC
189 -G--Q--L--G--L--D--S--I--K--D--Q--G--E--A--S--L--P--P--S--P--

625 CCCCATATCGGCAACGGCACGCCACAATCCCTACGATCCCGTTCGACCCATCGAT
209 -P--H--I--G--N--G--N--A--Y--N--P--Y--D--P--G--F--A--P--I--D--

685 GGATCCGGAGATTGGATTGCCGATTGACTCGACCACTACTTCAACAACCGAAC
229 -G--S--A--E--I--R--A--A--I--D--S--T--S--T--S--T--A--T--

745 ACCACGACGACAGCGTCCAGCTGAGCACCAACGGAAATGGACCTCGATCTACTG
249 -T--T--T--A--S--S--S--T--T--E--T--E--M--D--L--D--L--L--

805 AACGCACGCCGAGAACAGACCCAAACAAATTCCGGCAGTTGTCCGTGGAAGTGCAG
269 -N--A--P--P--Q--N--R--P--Q--T--I--S--G--S--C--P--W--K--C--E--

TM V: a.a.294-316

865 CTGACCAACGATCGGGGTTATGCCTGACTCCGCCCTGGGCTCATTCTATATACCATG
 289 -L--T--N--D--R--G--Y--V--L--Y--S--A--L--G--S--F--Y--I--P--M-

925 TTCGTGATGCTCTCTACTGGCGATCTACCGGGCTGCCGTGAGAACGACGAGAGCC
 309 -F--V--M--L--F--F--Y--W--R--I--Y--R--A--A--V--R--T--R--A-

MI12417> Coding intron 3; 3R:20,697,059**MI12417> Intracellular: a.a.338****Exon 4>3R:20,693,848-20,692,947**

985 ATCAACCAGGGCTTCAGACCACCAAGGGCAGTCCCCGAGTCGGCAACAATCGAGTG
 329 -I--N--Q--G--F--K--T--T--K--G--S--P--R--E--S--G--N--N--R--V-

1045 GACGAGTCCCAGCTCATATTGCGCATTACCGAGGAAGACCTTGCTCACCCCCCAGCGC
 349 -D--E--S--Q--L--I--L--R--I--H--R--G--R--P--C--S--T--P--Q--R-

1105 ACGCCCTCTGGTCACTCAATGCTCGACTCTCAGCGTGAACAGAACGGGGGGCGG
 369 -T--P--L--S--V--H--S--M--S--S--T--L--S--V--N--S--N--G--G--G-

1165 GGTGGAGCCGTGGCCTCGGGACTGGGTGCCTCCACCGAGGATCACCTCAGGGAGGC
 389 -G--G--A--V--A--S--G--L--G--A--S--T--E--D--H--L--Q--G--G--A-

1225 CCCAAGCGGGCACATCGATGCGCGTCTGCCGACAGCGACACGAGAAAGGTGGCCATCAAG
 409 -P--K--R--A--T--S--M--R--V--C--R--Q--R--H--E--K--V--A--I--K-

1285 GTGTCCTTCCCTCCGAGAAATGCTCGACGAGCAGCAGCACAGGCATCGCCA
 429 -V--S--F--P--S--S--E--N--V--L--D--A--G--Q--P--Q--A--S--P-

1345 CACTATGCGTAATCAGTAGCGCCAACGGACGTCGTGCCTCTTAAGACGAGCCTCTC
 449 -H--Y--A--V--I--S--S--A--N--G--R--R--A--S--F--K--T--S--L--F-

1405 GACATTGGCAGACCACCTTAATTGGACCGAGCTGCGTCCGGTCCGGAGACCTAGAG
 469 -D--I--G--E--T--T--F--N--L--D--A--A--A--S--G--P--G--D--L--E-

1465 ACCGGACTCTGACCACCTCACTGCGGCCAAGAACGGCAGGCAAGCGCAGCGCCAAG
 489 -T--G--L--S--T--S--L--S--A--K--K--R--A--G--K--R--S--A--K-

TM VI: a.a.524-546

1525 TTTCAGGTGAAGCGGTTCCGAATGGAGACCAAGGCAGCCAAGACGCTGGCCATATTG
 509 -F--Q--V--K--R--F--R--M--E--T--K--A--A--K--T--L--A--I--V-

1585 GGCGGCTTCATCGTTGCTGGCTGCCCTTCACTGATGTATCTGATCCGGGCTTCTGC
 529 -G--G--F--I--V--C--W--L--P--F--T--M--Y--I--R--A--F--C-

TM VII: a.a.556-578

1645 GACCACTGCATTAGCCGACGGTCTTTCGGTCTTCTGGCTGGCTACTGCAACTCG
 549 -D--H--C--I--Q--P--T--V--F--S--V--L--F--W--L--G--Y--C--N--S-

1705 GCCATTAATCGATGATCTATGCGCTTTCTCGAATGAGTTCGCATGCCCTCAAGCG
 569 -A--I--N--P--M--I--Y--A--L--F--S--N--E--F--R--I--A--F--K--R-

1765 ATAGTGTGAGATGCGTCTGCACCCGAGTGGCTCCGGCGTCGGAGAATTCCAGATG
 589 -I--V--C--R--C--V--C--T--R--S--G--F--R--A--S--E--N--F--Q--M-

1825 ATAGCGGGCGTGGCTGATGGCACCGAACATTCCACAAGACCATATCCGGATGCTG
 609 -I--A--A--R--A--L--M--A--P--A--T--F--H--K--T--I--S--G--C--S-

1885 GACGACGGCGAGGGCGTGGACTTCAGCTGA
 629 -D--D--G--E--G--V--D--F--S--*-

Supplementary Table S1.**Comparison of synapse numbers between sVUM1 neurons and postsynaptic neurons in the calyx in 1st and 3rd instar larvae.**

The number of synapses between sVUM1 neurons and other neurons in the calyx (KCs, APL, both Odd neurons together) for first instar larva were extracted from the online publicly available resource, Virtual Fly Brain, <https://catmaid.virtualflybrain.org/L1> Larval CNS (L1EM) (Licence CC-BY-SA_4.0). First instar data correspond to synaptic contacts judged by EM criteria, corresponding approximately to the numbers of active zones. These were obtained by using the connectivity tool to display all downstream neurons of OAN-a1/ sVUMmd1 or OAN-a2/ sVUMmx1, and exported as a csv file. Numbers indicate the total number of synapses per neuron type with both sVUM1s, in both brain hemispheres, for APL and Odds, extracted from the left and right annotations in the CATMAID database. For KCs, the numbers should be doubled as shown for consistency, since the numbers were manually calculated from the csv file by identifying the numbers of synapses corresponding to single KCs, and these were annotated only on one side of the brain, in the CATMAID database. Calyx sVUM1-PN synapses are not included, since these could not be distinguished in these lists from sVUM1-PN synapses in the AL. A breakdown of synapse numbers for individual neurons in first instar larvae is in Supplementary File 1.

Third instar data were taken from OA-positive GRASP puncta as described in the Results text of this work, and refer to one brain hemisphere only. For the purpose of comparisons, numbers must be doubled as indicated to represent values for both brain halves together. Examples are shown in Fig. 3. Notice almost double numbers of synapses at 3rd instar larval stage for KCs and Odd, while for APL, numbers at first instar are 11.6% of that at 3rd instar.

	KCs	Odd neurons	APL
1st instar KCs: one calyx only Odds and APL: left and right calyx together)	2 x 49 (n=1)	67 (n=1)	13 (n=1)
3rd instar (single calyx; double this number to estimate left and right calyx together)	2 x 96 ± 34 (n=3)	2 x 63 ± 3 (n=3)	2 x 56 ± 7 (n=4)

Supplementary Methods

Odor balancing. For learning experiments, we needed to determine concentrations of ethyl acetate (EA) or pentyl acetate (PA) that gave a preference index (Pref-I, defined in the main paper) close to zero in naive larvae, so that deviations from this score could be used as a measure of learning after conditioning with an appetitive stimulus.

We carried out initial balancing experiments using Canton-S (CS) to determine the range of dilutions of ethyl acetate (EA) or (PA) that were approximately equally attractive to larvae.

	Pref-I at 2 min	Pref-I at 5 min
EA 1:2000 vs PA 1:200	-0.14 ± 0.06 (n=16)	-0.41 ± 0.07 (n=16).
EA 1:2000 vs PA 1:500	-0.10 ± 0.04 (n=19)	-0.31 ± 0.05 (n=19).
EA 1:2000 vs PA 1:1000	-0.03 ± 0.07 (n=8)	-0.30 ± 0.09 (n=8).

Odor conditioning. We carried out fructose conditioning on CS larvae using EA at 1:2000 and PA at 1:500 dilutions, using white light and standard food. We recorded the Performance Index (PI) values for EA conditioning (EA+), and for PA conditioning (PA+) as defined in the main text, and used these to calculate Performance Index as a measure of learning. Counting of larvae was done at 2 min and 5 min in each test.

	PI (EA+)	PI (PA+)	PI (Learning)
2 min	0.27 ± 0.04 (n=18)	-0.27 ± 0.05 (n=18)	0.27 ± 0.04 (n=18)
5 min	0.28 ± 0.06 (n=18)	-0.52 ± 0.03 (n=18)	0.40 ± 0.04 (n=18).

We next used these concentrations to measure Pref-I values of larvae of the genotype used in Fig. 9 (n=8)

Light	Odors	Naive Pref-I
Blue	EA (1:2000) vs PA (1:500)	0.03 ± 0.06
Blue	EA:PA 1:4 vs EA:PA 4:1,	0.00 ± 0.04
Amber	EA:PA 1:4 vs EA:PA 4:1,	0.11 ± 0.03

Given the low naive Pref-I values measures with these odor concentrations, we used these for the learning and discrimination experiments reported in the main paper.